NJC

New Journal of Chemistry

An international journal of the chemical sciences

www.rsc.org/njc

Volume 33 | Number 2 | February 2009 | Pages 213–440

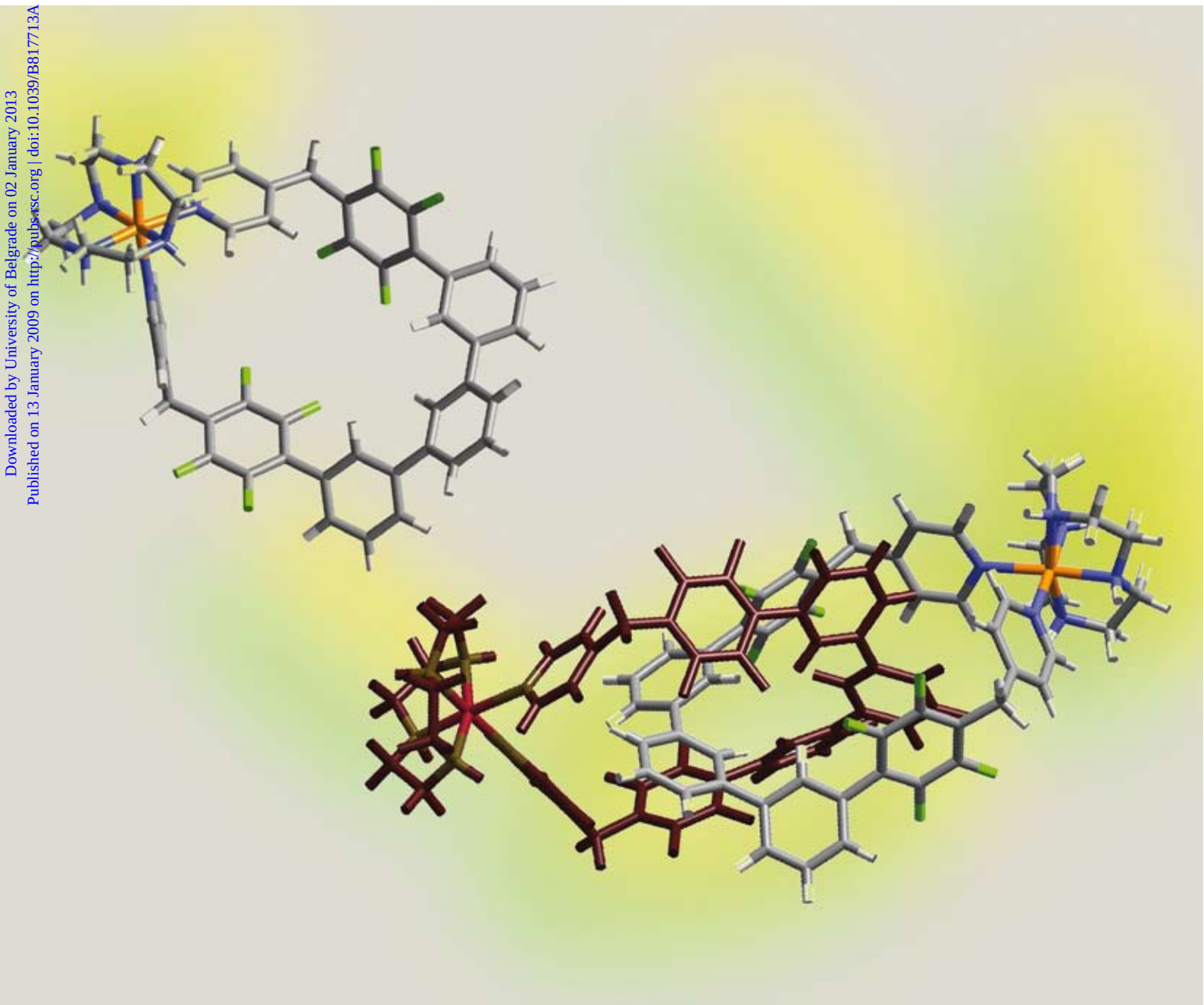

ISSN 1144-0546

RSC Publishing

PAPER

Makoto Fujita *et al.*

Photo-induced self-assembly of Pt(II)-linked rings and cages *via* the photolabilization of a Pt(II)–py bond

Photo-induced self-assembly of Pt(II)-linked rings and cages *via* the photolabilization of a Pt(II)–py bond†‡

Ken-ichi Yamashita,§ Kei-ichi Sato, Masaki Kawano and Makoto Fujita*

Received (in Montpellier, France) 8th October 2008, Accepted 28th November 2008
First published as an Advance Article on the web 13th January 2009
DOI: 10.1039/b817713a

An inert Pt(II)–pyridine bond is considerably labilized upon UV irradiation. On the basis of this phenomenon, kinetically inert Pt(II)-linked coordination rings and cages are formed in high yields from their components by obtaining a kinetically distributed mixture and subsequently equilibrating the mixture into the thermodynamically stable structures upon temporary photolabilization. This method is applicable when the pyridine rings in the ligands are not conjugated with other aromatic rings, in good agreement with DFT calculations that indicate the dependency of the photolability on the π-conjugation of the ligand frameworks. Interruption of π-conjugation either by introducing an methylene linker or by twisting the aromatic rings are effective to accomplish the photo-induced self-assembly.

Introduction

Molecular self-assembly is a simple and efficient methodology for the construction of large and complex architectures; *e.g.* macrocycles, interlocked compounds, helicates, grids, and hollow cages.[1,2] Typically, self-assembly is considered to be a thermodynamic phenomenon; that is, thermodynamically unfavorable products continuously reorganize until the most stable product(s) is (are) obtained.[3] Therefore, reversible bonds are essential to the thermodynamic proof-reading and reorganization.

The assembled architectures are, however, often unstable under forced conditions because of the reversibility of the coordination bonds. Though irreversible bonds are potentially capable of forming stable structures, they cannot reorganize and a complicated mixture of kinetic products are obtained. Recently, the turning on and off of reversible bonds by external stimuli is of considerable interest for controlling self-assembled architectures. Namely, designed structures assemble at the labilized "on" state and become stable at the "off" state. Several groups have successfully utilized dynamic covalent bonds for self-assembly.[4] In our work, the inert Pt(II)–pyridine coordination bond is a major focus.[5] The Pt(II)–pyridine bond is kinetically inert at room temperature, but becomes labile at elevated temperature (~100 °C). Platinum linked coordination rings, catenanes,[5a] and 3D cages[5b] have been self-assembled by prolonged heating. Once formed, the products are more stable than that of their Pd(II) analogues.

Herein, we show that the inert Pt(II)–pyridine bond can be labilized upon UV irradiation and applied to the photo-induced self-assembly of platinum linked molecular architectures through a "photoswitchable molecular lock" concept (Scheme 1).[6] To the best of our knowledge, self-assembly driven by photoirradiation has not been reported. Typically, covalent bonds undergo photochemical reactions involving structural changes or decomposition.[7] Coordination bonds are known to be photolabile, but have only been applied towards photoisomerization or photodissociation and not self-assembly.[8]

Results and discussion

Photo-induced self-assembly of Pt(II)-linked coordination rings

We first investigated the self-assembly of a simple diplatinum coordination ring **3a** composed of two ethylenediamine platinum(II) (enPt) corners and two bidentate pyridyl ligands (Fig. 1).[9] Photo-induced self-assembly was performed as follows: a room-temperature D_2O–1,4-dioxane-d_8 (1 : 1) solution containing (en)Pt$(NO_3)_2$ (**1**, 10 mM) and 1,2-bis(4-pyridyl)

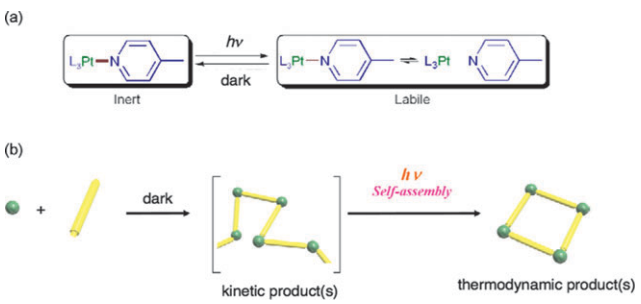

Scheme 1 (a) Photo-labilization of the Pt(II)–pyridine coordination bond.[6] (b) Schematic representation of photo-induced self-assembly.

Department of Applied Chemistry, School of Engineering, The University of Tokyo and CREST, Japan Science and Technology Corporation (JST), 7-3-1 Hongo, Bunkyo-ku, Tokyo 113-8656, Japan. E-mail: mfujita@appchem.t.u-tokyo.ac.jp; Fax: +81 3 5841 7257; Tel: +81 3 5841 7259

† Dedicated to Professor Jean-Pierre Sauvage on the occasion of his 65th birthday.

‡ Electronic supplementary information (ESI) available: Experimental details and spectroscopic data. CCDC reference number 704196. For ESI and crystallographic data in CIF or other electronic format see DOI: 10.1039/b817713a

§ Present address: Department of Chemistry, Graduate School of Science and Engineering, Tokyo Metropolitan University, 1-1 Minami-osawa, Hachioji, Tokyo 192-0397, Japan.

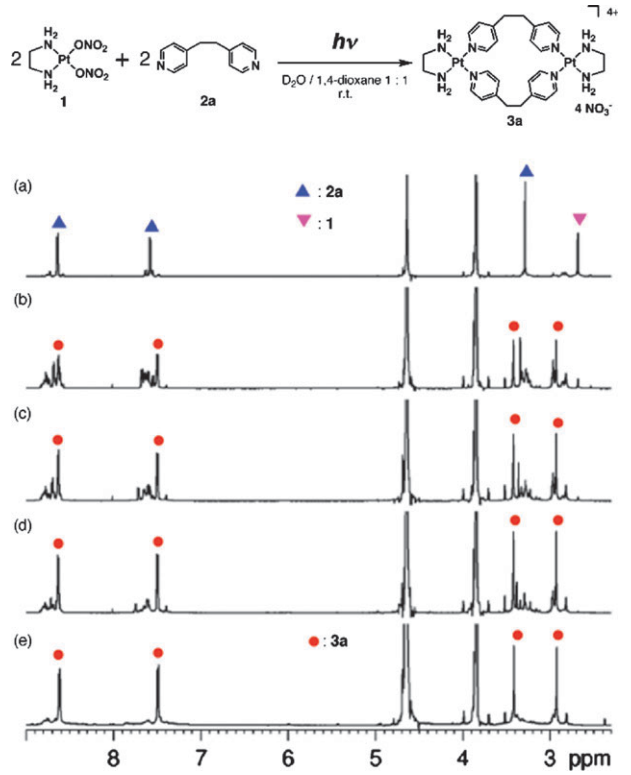

Fig. 1 ^{1}H NMR spectra of the photo-irradiation stimulated self-assembly of Pt(II)-linked macrocycle **3a** (500 MHz, D_2O–1,4-dioxane-d_8 1 : 1) at (a) t = 0, (b) t = 15 min, (c) t = 30 min, (d) t = 60 min and (e) t = 240 min.

ethane (**2a**, 10 mM) was irradiated with a filtered Hg–Xe lamp source by a band-path glass filter (330 ± 70 nm) and the reaction was monitored by ^{1}H NMR. Immediately after mixing, the signals for **1**, **2a** and a small amount of coordinated products were observed (Fig. 1(a)). Upon irradiation, signals for **1** and **2a** slowly disappeared and the new signals for macrocycle **3a** appeared and reached completion after 4 h (Fig. 1(e)). Cold-spray ionization mass spectrometry (CSI-MS) analysis[10] gave clear signals for the solvated macrocycle $([\mathbf{3a} - (NO_3^-)_m + (dmf)_n]^{m+}$ where m = 1–4 and n = 0–8) as well as the nearly naked macrocycle ($1064.2\ [\mathbf{3a} - NO_3^-]^+$) and clearly confirm the formation of **3a**. Without irradiation, the Pt(II)–pyridine bond formation is not reversible and clean formation of **3a** was not observed at room temperature. On heating the solution at 80 °C the Pt(II)–pyridine bond is activated but formation of **3a** still requires several days for completion. Similar conditions (but shorter reaction times) gave the larger macrocycles **3b** and **3c** (Scheme 2).[9] The photochemically driven self-assembly, however, is not general and when 4,4′-bipyridine (**4a**), 1,4-bis(4-pyridyl)benzene (**4b**),

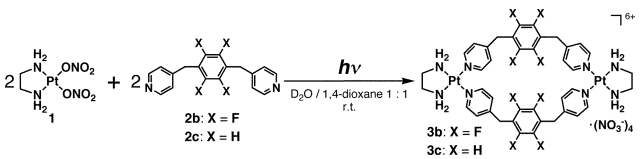

Scheme 2 Photo-induced self-assembly of Pt(II)-linked macrocycle **3b** and **3c**.

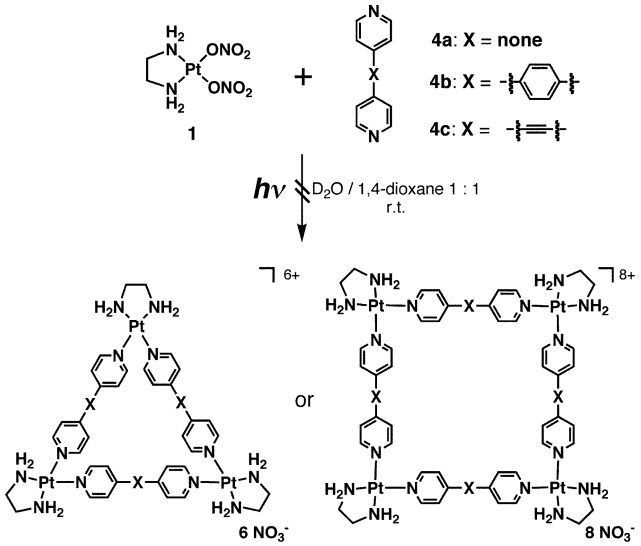

Scheme 3 Discrete structures were not formed by photo-induced self-assembly from ligand **4a**, **4b** and **4c**.

or 1,2-bis(4-pyridyl)acetylene (**4c**)[11] were irradiated in the presence of (en)Pt(NO_3)$_2$ (**1**), the initially formed polymeric products never reassembled into clear, discrete structures (Scheme 3).[5a,12]

Electronic structure calculations

Density functional theory (DFT) calculations were performed to help elucidate the structure–activity relationship (SAR) between the electronic structure of the complexes and the observed photolability (or lack thereof). DFT calculations of photo-inactive complexes $[(en)Pt(\mathbf{4a})]_4^{8+}$, $[(en)Pt(\mathbf{4b})]_3^{6+}$ and $[(en)Pt(\mathbf{4c})]_3^{6+}$ were carried out at the B3LYP level of the theory with the LANL2DZ basis sets for Pt, and 6-31G* basis sets for the other atoms. As previously reported,[6] the lability of platinum complexes stems from the $[(en)Pt(pyridine)_2]^{2+}$ and is due to excitation into the platinum antibonding $d_{x^2-y^2}$ orbital (Fig. 2(a)). The LUMOs of inactive complexes $[(en)Pt(\mathbf{4a})]_4^{8+}$, $[(en)Pt(\mathbf{4b})]_3^{6+}$ and $[(en)Pt(\mathbf{4c})]_3^{6+}$ are dominated by the π* orbitals of the ligands. The ligand π* orbitals are stabilized by the extended conjugation and lie energetically *below* the platinum antibonding $d_{x^2-y^2}$ orbital (Fig. 2(b)–(d)). Thus, photoexcitation occurs into the ligand π* orbital and has little effect on the stability of the platinum coordination bond. In the photoactive complexes **3a**, **3b** and **3c** the ligand π* orbitals lie energetically *above* the platinum antibonding $d_{x^2-y^2}$ orbital, photoexcitation occurs into the platinum antibonding $d_{x^2-y^2}$ orbital, and the coordination bond can dissociate.

Photo-induced self-assembly of rigid triangular and cage-like complexes from twisted aromatic ligands

According to the DFT calculations, raising the ligand LUMO energy by tuning the π-system should enhance photo-induced self-assembly. Methylene-linked pyridines provided a useful scaffold for macrocycle generation, but construction of larger structures is generally difficult due to the greater degree of conformation freedom. Rigid aromatic ligands, *i.e.*, **4b**, are

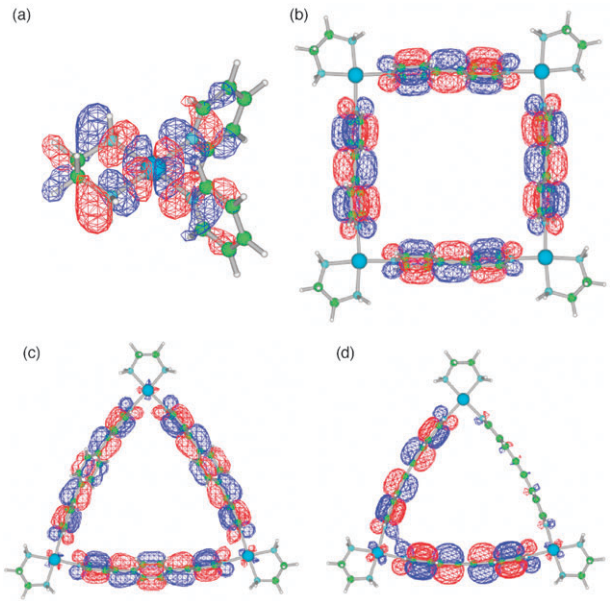

Fig. 2 DFT-calculated LUMOs for (a) $[(en)Pt(pyridine)_2]^{2+}$, (b) square complex $[(en)Pt(\mathbf{4a})]_4^{8+}$, (c) triangle complexes $[(en)Pt(\mathbf{4b})]_3^{6+}$ and (d) $[(en)Pt(\mathbf{4c})]_3^{6+}$.

well-suited to the construction of supramolecular architectures but feature extended π-conjugation between pyridine rings and the central phenylene ring and form photo-inactive platinum complexes. Conjugation between aromatic rings depends on orbital overlap and is reduced when the aromatic backbone is twisted.[13] The twisted ligand **4d**, where the extended π-system is disrupted by the enforced orthogonality of the duryl group (Fig. 3), was thus designed. DFT calculations for the potential triangular product **5** were performed and, as expected, the LUMO is dominated by the antibonding $d_{x^2-y^2}$ orbital (Fig. 4).

Accordingly, the photo-induced self-assembly of **5** from ligand **4d** was examined. Ligand **4d** was easily synthesized by the Suzuki–Miyaura cross-coupling of commercially available 1,4-diiodo-2,3,5,6-tetramethylbenzene with 4-(4,4,5,5-tetramethyl-1,3,2-dioxaborolan-2-yl)pyridine. Photo-induced self-assembly was performed as follows: a D_2O–1,4-dioxane-d_8

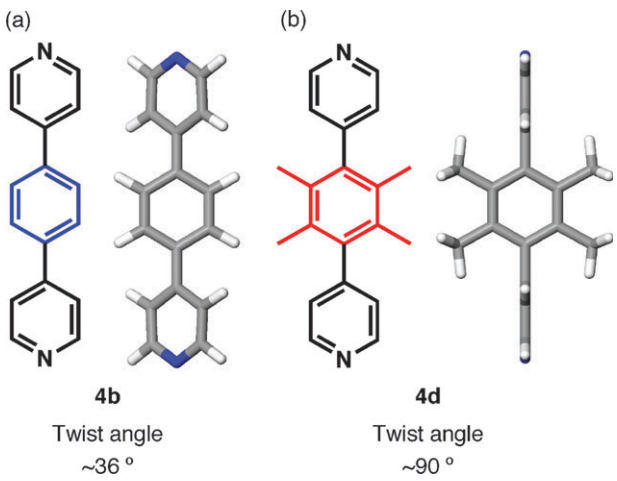

Fig. 3 Chemical and DFT-calculated structures of (a) **4b** and (b) **4d**.

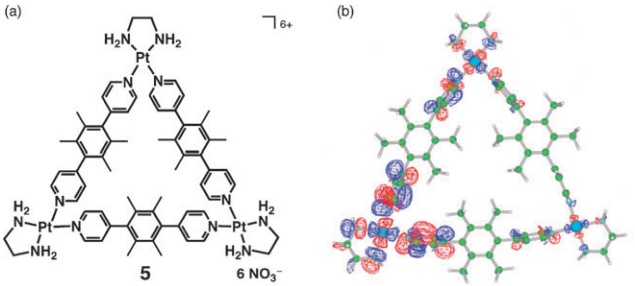

Fig. 4 (a) Chemical structure of expected self-assembled triangle product **5** and (b) the LUMO diagram.

(1 : 1) solution of $(en)Pt(NO_3)_2$ (**1**) and ligand **4d** was irradiated at room temperature (Fig. 5). As expected, the triangular complex **5** gradually formed upon irradiation. The reaction reached completion after 4 h and triangular complex **5** and a minor amount of the square complex were obtained.[14] The triangular complex selectively crystallized upon evaporation and X-ray crystallographic analysis confirmed the expected triangular structure (Fig. 6).

The tridentate ligand **6** was next prepared for the photo-induced self-assembly of a 3D cage complex **7** with a M_6L_4 stoichiometry (Fig. 7).[15] Cage complex **7** selectively self-assembled when a D_2O–1,4-dioxane-d_8 solution of **1** and **6** (in 6 : 4 molar ratio) was irradiated for 2 h (Fig. 7). In the ^1H NMR spectrum of **7**, methyl groups inside and outside the cage were independently observed because the rotatory motion of methyl-attached phenylene rings was sterically restricted (Fig. 7(d)). The CSI-MS spectrum of **7** in H_2O–1,4-dioxane–DMF (1 : 1 : 0.1) showed clear signals for the solvated cage $([\mathbf{7} - (NO_3^-)_m + (dmf)_n]^{m+}$ where m = 5–10 and n = 0–17) in addition to the unsolvated cage ($[\mathbf{7} - (NO_3^-)_5]^{5+}$) (Fig. 8).

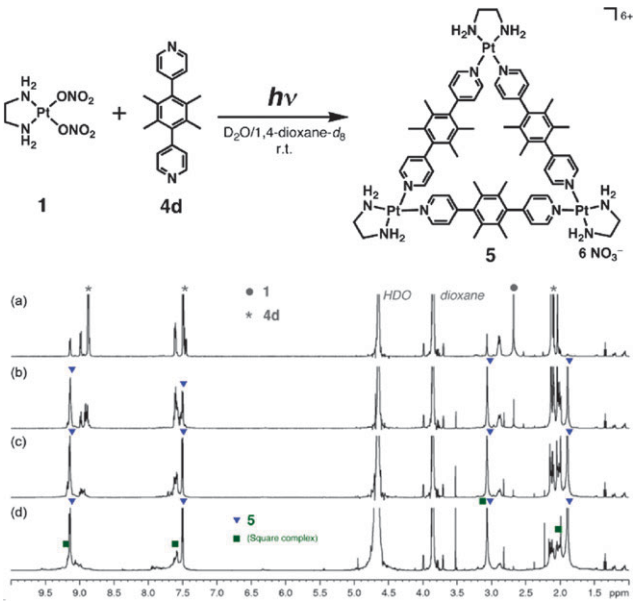

Fig. 5 ^1H NMR spectra of the photo-induced self-assembly of Pt(II)-linked triangular complex **5** (500 MHz, D_2O–1,4-dioxane-d_8 1 : 1) at (a) t = 0, (b) t = 15 min, (c) t = 30 min, (d) t = 60 min and (e) t = 240 min.

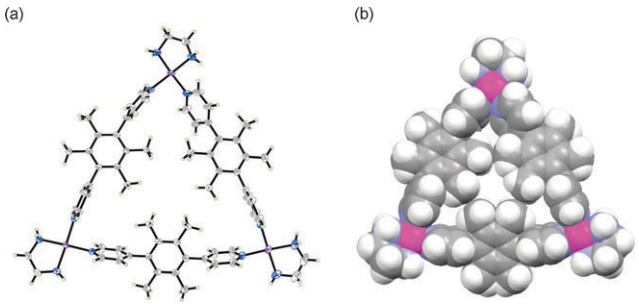

Fig. 6 The crystal structure of **5** in the (a) ORTEP view with 50% probability ellipsoids and (b) space-filling representation. Solvent molecules and counter anions are omitted for clarity.

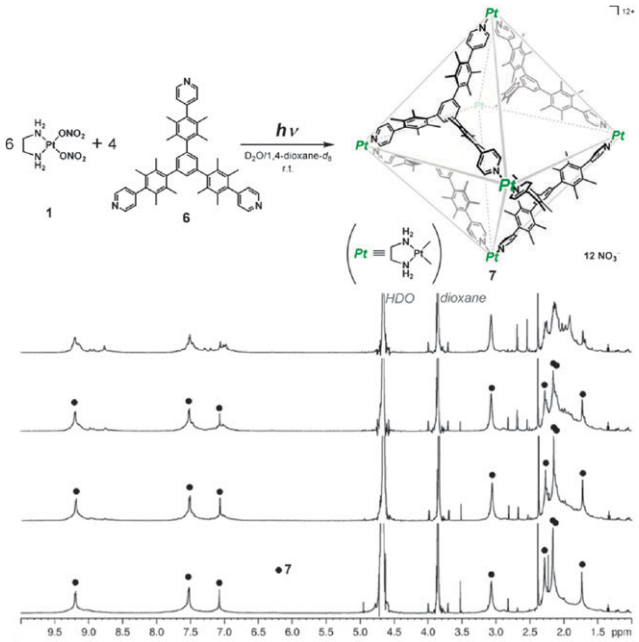

Fig. 7 ^{1}H NMR spectra of the photo-induced self-assembly of Pt(II)-linked cage complex **7** (500 MHz, D_2O–1,4-dioxane-d_8 1 : 1) at (a) $t = 0$, (b) $t = 30$ min, (c) $t = 60$ min and (d) $t = 120$ min.

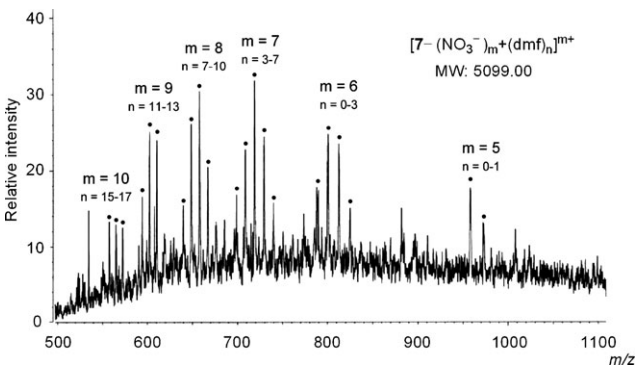

Fig. 8 CSI-MS spectrum of **7** as a solution in H_2O–1,4-dioxane–DMF (1 : 1 : 0.1).

The cage structure **7** was calculated and the diagonal Pt–Pt distances were estimated to be 2.9 nm (Fig. 9).

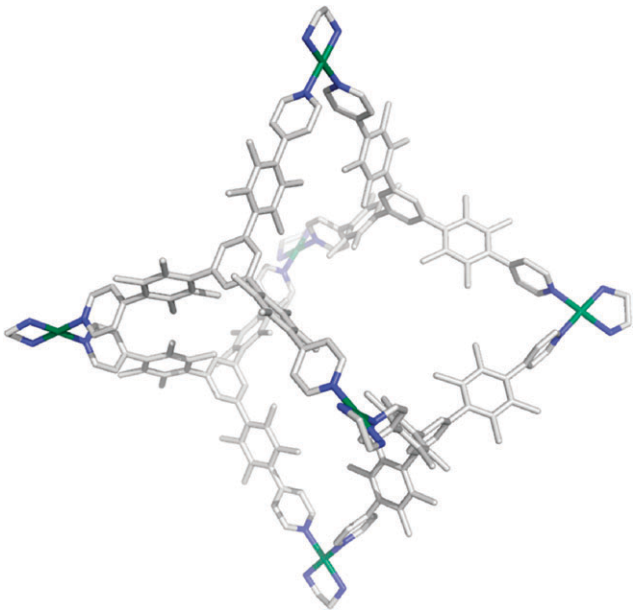

Fig. 9 Geometry optimized structure of the Pt(II)-linked cage complex **7** by using Accelrys's program "Forcite" with force field "Universal" on Materials Studio 4.0. Hydrogen atoms are omitted for clarity.

Conclusion

In conclusion, photo-induced self-assembly of Pt(II) containing macrocyclic or cage structures have been achieved based on the temporary labilization of Pt(II)–pyridine bonds. The photolability of the complexes can be tuned by controlling the energy of pyridyl ligand LUMO and be predicted by DFT calculations. To the best of our knowledge, this is the first example of self-assembly driven by photo-irradiation.

Experimental

General

Ligand **2b**,[9] **2c**,[9] **4b**,[11] **4c**[11] and 1,3,5-tris(4,4,5,5-tetramethyl-1,3,2-dioxaborolan-2-yl)benzene[16] were synthesized according to previously reported procedures. All other chemicals were of reagent grade and used without any further purification. D_2O, 1,4-dioxane-d_8 and $CDCl_3$ were acquired from Cambridge Isotopic Laboratories, Inc.

All NMR spectral data were recorded on a Bruker DRX-500 (500 MHz) spectrometer or Bruker AXL-500 (500 MHz) spectrometer. These data were collected at ambient temperature (300 K) unless otherwise noted and the chemical shift values reported here were with respect to the TMS ($CDCl_3$ solution) standard. EI-MS data were measured on Agilent Technologies 5973N spectrometer. MADLI-TOF MS data were measured on Applied Biosystems Voyager DE-STR. CSI-MS (Coldspray ionization mass spectroscopy) data were measured on a four-sector (BE/BE) tandem mass spectrometer (JMS-700C, JEOL) equipped with the CSI source. IR measurements were carried out as KBr pellets using a DIGILAB Scimitar FTS2000 instrument. UV-Vis spectral data were recorded on SHIMADZU UV-3150 spectrometer.

Melting points were determined on a Yanaco MF-500 V melting point apparatus. UV-irradiation was used with a SAN-EI UVF-203S Hg–Xe lamp filtered by a band-path glass filter (330 ± 70 nm, UV-D33S; Toshiba) and water filter (optical path: 3 cm).

DFT calculations were carried out using the Gaussian 03 program package.[17] The structure was optimized using the B3LYP level of the theory with the LANL2DZ basis sets for Pt, and 6-31G* basis set for the other atoms.

Syntheses

2,3,5,6-Tetramethyl-1,4-bis(pyridin-4-yl)benzene (4d). 1,4-Diiodo-2,3,5,6-tetramethylbenzene (386 mg, 1 mmol), 4-(4,4,5,5-tetramethyl-1,3,2-dioxaborolan-2-yl)pyridine (615 mg, 3 mmol), K_2CO_3 (1.38 g, 10 mmol), $Pd(PPh_3)_4$ (231 mg, 0.2 mmol) were mixed in degassed DMF (20 mL), and stirred at 90 °C under argon for 24 h. Solvent was removed under reduced pressure, and the residue was poured into water and extracted with $CHCl_3$. The organic layer was washed with water and brine, and dried over $MgSO_4$, followed by the removal of the solvent under reduced pressure. The crude product was purified by column chromatography (silica gel, CH_2Cl_2, then CH_2Cl_2–MeOH 50 : 1), followed by recrystallization from ethyl acetate to give **4d** as a white powder (233 mg, yield; 81%); mp >210 °C (sublimed); ^{1}H NMR (500 MHz, $CDCl_3$, r.t.) δ (ppm) = 8.70 (dd, J = 6.0 Hz, 1.6 Hz, 4H, PyH_α), 7.13 (dd, J = 6.0 Hz, 1.6 Hz, 4H, PyH_β), 1.93 (s, 12H, *Me*). ^{13}C NMR (125 MHz, $CDCl_3$, r.t.) δ (ppm) = 150.7 (C_q), 150.1 (*C*H), 139.3 (C_q), 131.4 (C_q), 124.8 (*C*H), 17.9 (*C*H$_3$). EI-MS; m/z = 288 [**4d**]$^+$. IR (KBr, cm^{-1}); 3028, 2927 (br), 1593, 1542, 1408, 1215, 1070, 988, 870, 812, 753, 640. Elemental analysis: calc. for $C_{20}H_{20}N_2$: C, 83.30; H, 6.99; N, 9.71; found: C, 83.03; H, 7.11; N, 9.51%.

4-(4-Iodo-2,3,5,6-tetramethylphenyl)pyridine. 1,4-Diiodo-2,3,5,6-tetramethylbenzene (4.63 g, 12 mmol), 4-(4,4,5,5-tetramethyl-1,3,2-dioxaborolan-2-yl)pyridine (820 mg, 4 mmol), K_2CO_3 (6.68 g, 48.3 mmol), $Pd(PPh_3)_4$ (462 mg, 0.4 mmol) were mixed in degassed DMF (50 mL), and stirred at 90 °C under argon for 10 h. Solvent was removed under reduced pressure, and the residue was poured into water and extracted with $CHCl_3$. The organic layer was washed with water and brine, and dried over $MgSO_4$, followed by the removal of the solvent under reduced pressure. The crude product was purified by column chromatography (silica gel, hexane–CH_2Cl_2 1 : 1, then CH_2Cl_2) to give the title compound as a white powder (1.16 g, yield; 86%); mp 192–193 °C; ^{1}H NMR (500 MHz, $CDCl_3$, r.t.) δ (ppm) = 8.67 (dd, J = 6.0 Hz, 1.6 Hz, 2H, PyH_α), 7.06 (dd, J = 6.0 Hz, 1.6 Hz, 2H, PyH_β), 2.55 (s, 6H, *Me*), 1.98 (s, 6H, *Me*). ^{13}C NMR (125 MHz, $CDCl_3$, r.t.) δ (ppm) = 150.4 (C_q), 150.1 (*C*H), 139.5 (C_q), 137.9 (C_q), 131.7 (C_q), 124.6 (*C*H), 111.7 (C_q), 27.8 (*C*H$_3$) 19.8 (*C*H$_3$). EI-MS; m/z = 337 [M]$^+$. IR (KBr, cm^{-1}); 3005, 2916 (br), 1593, 1541, 1444, 1409, 1382, 1223, 1213, 1070, 987, 862, 811, 641, 611. Elemental analysis: calc. for $C_{15}H_{16}NI$: C, 53.43; H, 4.78; N, 4.15; found: C, 53.38; H, 4.88; N, 3.93%.

1,3,5-Tris[2,3,5,6-tetramethyl-4-(pyridin-4-yl)phenyl]benzene (6). 4-(4-Iodo-2,3,5,6-tetramethylphenyl)pyridine (910 mg, 2.7 mmol), 1,3,5-tris(4,4,5,5-tetramethyl-1,3,2-dioxaborolan-2-yl)-benzene (274 mg, 0.6 mmol), K_2CO_3 (1.24 g, 9.0 mmol), $Pd(PPh_3)_4$ (208 mg, 0.18 mmol) were mixed in degassed DMF (30 mL), and stirred at 90 °C under argon for 24 h. Solvent was removed under reduced pressure, and the residue was poured into water and extracted with $CHCl_3$. The organic layer was washed with water and brine, and dried over $MgSO_4$, followed by the removal of the solvent under reduced pressure. The crude product was purified by column chromatography (silica gel, CH_2Cl_2 then CH_2Cl_2–MeOH 30 : 1) to give **6** as white solid (309 mg, yield; 78%); mp 177–179 °C; ^{1}H NMR (500 MHz, $CDCl_3$, r.t.) δ (ppm) = 8.69 (d, J = 5.8 Hz, 6H, PyH_α), 7.13 (d, J = 5.8 Hz, 6H, PyH_β), 7.00 (s, 3H, Ph*H*), 2.17 (s, 18H, *Me*), 1.95 (s, 18H, *Me*). ^{13}C NMR (125 MHz, $CDCl_3$, r.t.) δ (ppm) = 151.2 (C_q), 150.0 (*C*H), 142.7 (C_q), 141.8 (C_q), 138.5 (C_q), 132.0 (C_q), 130.9 (C_q), 128.7 (*C*H), 125.0 (*C*H), 18.1 (*C*H$_3$), 18.0 (*C*H$_3$). MALDI-TOF MS (dithranol matrix); m/z = 706 [**6** + H]$^+$. IR (KBr, cm^{-1}); 2990, 2922 (br), 1596, 1541, 1457, 1409, 1204, 1132, 1013, 990, 896, 855, 812, 788, 640, 616.

Pt(II)-linked ring 3a. A D_2O solution (0.5 mL) of (en)$Pt(NO_3)_2$ (**1**, 3.79 mg, 0.01 mmol) was added to a 1,4-dioxane-d_8 (0.5 mL) solution of 1,2-bis(4-pyridyl)ethane (**2a**, 1.84 mg, 0.01 mmol), and the solution was put in the UV quarts cell and irradiated at room temperature under aerobic condition. The reaction was monitored by ^{1}H NMR, and **3a** was almost quantitatively formed after 4 h. ^{1}H NMR (500 MHz, D_2O–1,4-dioxane-d_8 1 : 1, r.t.) δ (ppm) = 8.63 (d, J = 6.5 Hz, 8H, PyH_α), 7.50 (d, J = 6.5 Hz, 8H, PyH_β), 3.42 (s, 8H, CH_2), 2.93 (s, 8H, *en*). ^{13}C NMR (125 MHz, D_2O–1,4-dioxane-d_8 1 : 1, r.t.) δ (ppm) = 154.6 (C_q), 151.5 (*C*H), 127.5 (C_q), 47.6 (*en*), 33.0 (*C*H$_2$). CSI-MS (H_2O–MeOH–DMF): m/z = 329.1 [**3a** − $(NO_3^-)_4$ + $(dmf)_6]^{4+}$, 347.3 [**3a** − $(NO_3^-)_4$ + $(dmf)_7]^{4+}$, 365.6 [**3a** − $(NO_3^-)_4$ + $(dmf)_8]^{4+}$, 410.7 [**3a** − $(NO_3^-)_3$ + $(dmf)_4]^{3+}$, 435.1 [**3a** − $(NO_3^-)_3$ + $(dmf)_5]^{3+}$, 459.4 [**3a** − $(NO_3^-)_3$ + $(dmf)_6]^{3+}$, 483.7 [**3a** − $(NO_3^-)_3$ + $(dmf)_7]^{3+}$, 501.1 [**3a** − $(NO_3^-)_2]^{2+}$, 537.6 [**3a** − $(NO_3^-)_2$ + dmf]$^{2+}$, 574.1 [**3a** − $(NO_3^-)_2$ + $(dmf)_2]^{2+}$, 610.6 [**3a** − $(NO_3^-)_2$ + $(dmf)_3]^{2+}$, 647.1 [**3a** − $(NO_3^-)_2$ + $(dmf)_4]^{2+}$, 1064.2 [**3a** − $NO_3^-]^+$.

Pt(II)-linked ring 3b. A D_2O solution (0.5 mL) of (en)$Pt(NO_3)_2$ (**1**, 3.79 mg, 0.01 mmol) was added to a 1,4-dioxane-d_8 (0.5 mL) solution of 2,3,5,6-tetrafluoro-1,4-bis-(4-pyridylmethyl)benzene (**2b**, 3.32 mg, 0.01 mmol), and the solution was put in the UV quarts cell and irradiated at room temperature under aerobic conditions. The reaction was monitored by ^{1}H NMR, and **3b** was almost quantitatively formed after 3 h. ^{1}H NMR (500 MHz, D_2O–1,4-dioxane-d_8 1 : 1, r.t.) δ (ppm) = 8.93 (d, J = 6.6 Hz, 8H, PyH_α), 7.63 (d, J = 6.6 Hz, 8H, PyH_β), 4.44 (s, 8H, CH_2), 2.96 (s, 8H, *en*). ^{13}C NMR (125 MHz, D_2O–1,4-dioxane-d_8 1 : 1, r.t.) δ (ppm) = 152.3 (*C*H), 152.1 (C_q), 145.2 (d, J = 241 Hz, *C*F), 127.1 (*C*H), 115.6 (*C*H), 47.7 (*en*), 27.3 (*C*H$_2$). CSI-MS (H_2O–MeOH–DMF): m/z = 403.3 [**3b** − $(NO_3^-)_4$ + $(dmf)_6]^{4+}$, 421 [**3b** − $(NO_3^-)_4$ + $(dmf)_7]^{4+}$, 439.8 [**3b** − $(NO_3^-)_4$ + $(dmf)_8]^{4+}$, 509.7 [**3b** − $(NO_3^-)_3$ + $(dmf)_4]^{3+}$, 534.1 [**3b** − $(NO_3^-)_3$ + $(dmf)_5]^{3+}$, 558.4 [**3b** − $(NO_3^-)_3$ + $(dmf)_6]^{3+}$, 649.6 [**3b** − $(NO_3^-)_2]^{2+}$, 686.1 [**3b** − $(NO_3^-)_2$ + dmf]$^{2+}$, 722.6 [**3b** − $(NO_3^-)_2$ + $(dmf)_2]^{2+}$, 1361.2 [**3b** − $NO_3^-]^+$.

Pt(II)-linked ring 3c. A D_2O solution (0.5 mL) of (en)Pt$(NO_3)_2$ (**1**, 3.79 mg, 0.010 mmol) was added to a 1,4-dioxane-d_8 (0.5 mL) solution of 1,4-bis(4-pyridylmethyl)benzene (**2c**, 2.60 mg, 0.010 mmol), and the solution was put in the UV quarts cell and irradiated at room temperature under aerobic condition. The reaction was monitored by ^{1}H NMR, and **3c** was almost quantitatively formed after 1.5 h. ^{1}H NMR (500 MHz, D_2O–1,4-dioxane-d_8 1 : 1, r.t.) δ (ppm) = 8.81 (d, J = 6.4 Hz, 8H, PyH_α), 7.59 (d, J = 6.4 Hz, 8H, PyH_β), 7.39 (s, 8H, Ph*H*), 4.26 (s, 8H, CH_2), 2.95 (s, 8H, *en*). ^{13}C NMR (125 MHz, D_2O–1,4-dioxane-d_8 1 : 1, r.t.) δ (ppm) = 155.8 (C_q), 151.8 (*C*H), 136.6 (C_q), 130.1 (*C*H), 127.5 (*C*H), 47.7 (*en*), 40.1 (*C*H$_2$). CSI-MS (H_2O–1,4-dioxane–DMF): m/z = 294.3 [**3c** – $(NO_3^-)_4$ + $(dmf)_2]^{4+}$, 312.5 [**3c** – $(NO_3^-)_4$ + $(dmf)_3]^{4+}$, 330.8 [**3c** – $(NO_3^-)_4$ + $(dmf)_4]^{4+}$, 345.2 [**3c** – $(NO_3^-)_4$ + $(dmf)_5]^{4+}$, 388.6 [**3c** – $(NO_3^-)_3$ + dmf]$^{3+}$, 413.0 [**3c** – $(NO_3^-)_3$ + $(dmf)_2]^{3+}$, 437.3 [**3c** – $(NO_3^-)_3$ + $(dmf)_3]^{3+}$, 461.3 [**3c** – $(NO_3^-)_3$ + $(dmf)_4]^{3+}$, 577.3 [**3c** – $(NO_3^-)_2]^{2+}$, 413.0 [**3c** – (NO_3^-)]$^+$.

Pt(II)-linked triangle 5. A D_2O solution (0.5 mL) of (en)Pt$(NO_3)_2$ (**1**, 3.79 mg, 0.010 mmol) was added to a 1,4-dioxane-d_8 (0.5 mL) solution of 2,3,5,6-tetramethyl-1,4-bis-(4-pyridyl)benzene (**4d**, 2.88 mg, 0.010 mmol), and the solution was put in the UV quarts cell and irradiated at room temperature under aerobic condition. The reaction was monitored by ^{1}H NMR, and **5** and a small amount of square complexes were formed after 3 h. Single crystals of **5** suitable for X-ray analysis were obtained by slow evaporation of solvent from a resulting solution of **5** at room temperature. ^{1}H NMR (500 MHz, D_2O–1,4-dioxane-d_8 1 : 1, r.t.) δ (ppm) = 9.14 (d, J = 6.7 Hz, 12H, PyH_α), 7.50 (d, J = 6.7 Hz, 12H, PyH_β), 3.07 (s, 8H, *en*), 1.89 (s, 36H, *Me*). ^{13}C NMR (125 MHz, D_2O–1,4-dioxane-d_8 1 : 1, r.t.) δ (ppm) = 154.8 (C_q), 152.5 (*C*H), 138.2 (C_q), 131.2 (C_q), 128.4 (*C*H), 36.7 (*en*), 17.9 (*C*H$_3$). CSI-MS (H_2O–1,4-dioxane–DMF): m/z = 393.7 [5 – $(NO_3^-)_6$ + $(dmf)_{10}]^{6+}$, 405.8 [**5** – $(NO_3^-)_6$ + $(dmf)_{11}]^{6+}$, 418.0 [**5** – $(NO_3^-)_6$ + $(dmf)_{12}]^{6+}$, 440.9 [**5** – $(NO_3^-)_5$ + $(dmf)_7]^{5+}$, 455.5 [**5** – $(NO_3^-)_5$ + $(dmf)_8]^{5+}$, 470.1 [**5** – $(NO_3^-)_5$ + $(dmf)_9]^{5+}$, 511.8 [**5** – $(NO_3^-)_4$ + $(dmf)_4]^{4+}$, 530.1 [**5** – $(NO_3^-)_4$ + $(dmf)_5]^{4+}$, 548.3 [**5** – $(NO_3^-)_4$ + $(dmf)_6]^{4+}$, 629.9 [**5** – $(NO_3^-)_3$ + dmf]$^{3+}$, 654.3 [**5** – $(NO_3^-)_3$ + $(dmf)_2]^{3+}$.

Pt(II)-linked cage 7. A D_2O solution (0.5 mL) of (en)Pt$(NO_3)_2$ (**1**, 2.28 mg, 0.006 mmol) was added to a 1,4-dioxane-d_8 (0.5 mL) solution of ligand **6** (2.82 mg, 0.004 mmol), and the solution was heated at 90 °C for 1 min to dissolve the component. The resultant solution was put in the UV quarts cell and irradiated at room temperature under aerobic condition. The reaction was monitored by ^{1}H NMR, and **7** was formed after 2 h. ^{1}H NMR (500 MHz, D_2O–1,4-dioxane-d_8 1 : 1, r.t.) δ (ppm) = 9.19 (d, J = 5.8 Hz, 24H, PyH_α), 7.52 (d, J = 6.2 Hz, 24H, PyH_β), 7.07 (s, 12H, Ph*H*), 3.06 (s, 24H, *en*), 2.28 (s, 12H, *Me*), 2.22 (s, 24H, 2 × *Me*), 1.73 (s, 12H, *Me*). CSI-MS (H_2O–1,4-dioxane–DMF): m/z = 557.8 [**7** – $(NO_3^-)_{10}$ + $(dmf)_{15}]^{10+}$, 565.1 [**7** – $(NO_3^-)_{10}$ + $(dmf)_{16}]^{10+}$, 572.2 [**7** – $(NO_3^-)_{10}$ + $(dmf)_{17}]^{10+}$, 594.1 [**7** – $(NO_3^-)_9$ + $(dmf)_{11}]^{9+}$, 602.3 [**7** – $(NO_3^-)_9$ + $(dmf)_{12}]^{9+}$, 610.4 [**7** – $(NO_3^-)_9$ + $(dmf)_{13}]^{9+}$, 639.5 [**7** – $(NO_3^-)_8$ + $(dmf)_7]^{8+}$, 648.7 [**7** – $(NO_3^-)_8$ + $(dmf)_8]^{8+}$, 657.8 [**7** – $(NO_3^-)_8$ + $(dmf)_9]^{8+}$, 666.9 [**7** – $(NO_3^-)_8$ + $(dmf)_{10}]^{8+}$, 708.5 [**7** – $(NO_3^-)_7$ + $(dmf)_4]^{7+}$, 718.9 [**7** – $(NO_3^-)_7$ + $(dmf)_5]^{7+}$, 729.5 [**7** – $(NO_3^-)_7$ + $(dmf)_6]^{7+}$, 739.8 [**7** – $(NO_3^-)_7$ + $(dmf)_7]^{7+}$, 787.7 [**7** – $(NO_3^-)_6]^{6+}$, 800.2 [**7** – $(NO_3^-)_6$ + dmf]$^{6+}$, 812.4 [**7** – $(NO_3^-)_6$ + $(dmf)_2]^{6+}$, 824.9 [**7** – $(NO_3^-)_6$ + $(dmf)_3]^{6+}$, 957.9 [**7** – $(NO_3^-)_5]^{5+}$, 972.1 [**7** – $(NO_3^-)_5{}^{5+}$ + dmf]$^{5+}$

Crystallography

Single-crystal XRD data for **5** was collected with a BRUKER SMART APEX II Ultra/TBN diffractometer with Mo-Kα radiation. The data were corrected for absorption with the SADABS program. SHELXTL-97 was used for structure solution and refinement. Because nitrate anions and water showed severe disorder, the geometric parameters were restrained. Non-hydrogen atoms were refined anisotropically and all hydrogen atoms for methyl groups were refined as a rigid group and the rest of hydrogen atoms were fixed at calculated positions and refined using a riding model.

Crystal data for 5. $C_{66}H_{123}N_{18}O_{37.5}Pt_3$, M_r = 2354.09, triclinic, $P\bar{1}$, a = 13.8836(18), b = 18.679(3), c = 19.283(3) Å, α = 92.901(2), β = 94.205(2), γ = 100.971(2)°, V = 4885.4(11) Å^3, Z = 2, T = 80(2) K, D_c = 1.6000 g cm^{-3}, λ(Mo-Kα) = 0.71073 Å; 56156 reflections were measured of which 22988 unique (R_{int} = 0.0229) were used in all calculations. The structure was solved by direct method (SHELXL-97) and refined by full-matrix least-squares methods on F^2 with 1403 parameters; R_1 = 0.0383 ($I > 2\sigma(I)$) and wR_2 = 0.0476, GOF = 1.040, max./min. residual density 3.041/−2.0193 e Å^{-3}.

References

1 (*a*) J. L. Atwood, J. E. D. Davies, D. D. Macnicol and F. Vögtle, *Comprehensive Supramolecular Chemistry*, Pergamon, Oxford, 1996, vol. 9; (*b*) J.-M. Lehn, *Supramolecular Chemistry Concepts and Perspectives*, VCH, Weinheim, 1995; (*c*) J. A. McCleverty and T. J. Meyer, *Comprehensive Coordination Chemistry II*, Pergamon, Oxford, 2004, vol. 7.

2 (*a*) M. Fujita, *Chem. Soc. Rev.*, 1998, **27**, 417; (*b*) M. Fujita, K. Umemoto, M. Yoshizawa, N. Fujita, T. Kusukawa and K. Biradha, *Chem. Commun.*, 2001, 509; (*c*) M. Fujita, M. Tominaga, A. Hori and B. Therren, *Acc. Chem. Res.*, 2005, **38**, 371.

3 (*a*) D. Philp and J. F. Stoddart, *Synlett*, 1991, 445; (*b*) G. M. Whitesides, J. P. Mathias and C. T. Seto, *Science*, 1991, **254**, 1312.

4 S. J. Rowan, S. J. Cantrill, G. R. L. Cousins, J. K. M. Sanders and J. F. Stoddart, *Angew. Chem., Int. Ed.*, 2002, **41**, 898.

5 (*a*) M. Fujita, F. Ibukuro, K. Yamaguchi and K. Ogura, *J. Am. Chem. Soc.*, 1995, **117**, 4175; (*b*) F. Ibukuro, T. Kusukawa and M. Fujita, *J. Am. Chem. Soc.*, 1998, **120**, 8561.

6 K. Yamashita, M. Kawano and M. Fujita, *J. Am. Chem. Soc.*, 2007, **129**, 1850.

7 (*a*) R. S. H. Liu, *Acc. Chem. Res.*, 2001, **34**, 555; (*b*) C. G. Bochet, *J. Chem. Soc., Perkin Trans. 1*, 2002, 125.

8 (*a*) P. Mobian, J.-M. Kern and J.-P. Sauvage, *Angew. Chem., Int. Ed.*, 2004, **43**, 2392; (*b*) J.-P. Collin and J.-P. Sauvage, *Chem. Lett.*, 2005, **34**, 742.

9 Pd(II) analogues of **3a** and **3b** have been reported previously: M. Fujita, S. Nagao, M. Iida, K. Ogata and K. Ogura, *J. Am. Chem. Soc.*, 1993, **115**, 1574.

10 S. Sakamoto, M. Fujita, K. Kim and K. Yamaguchi, *Tetrahedron*, 2000, **56**, 955.

11 Self-assembly from ligand **4b** or **4c** and (en)Pd units has been reported: M. Fujita, O. Sasaki, T. Mitsuhashi, T. Fujita, J. Yazaki, K. Yamaguchi and K. Ogura, *Chem. Commun*., 1996, 1535.
12 For a square complex composed of 4,4′-bipyridine and (en)Pd units; see: M. Fujita, J. Yazaki and K. Ogura, *J. Am. Chem. Soc*., 1990, **112**, 5645.
13 (*a*) G. Brizius, K. Billingsley, M. D. Smith and U. H. F. Bunz, *Org. Lett*., 2003, **5**, 3951; (*b*) P. P. Lainé, I. Ciofini, P. Ochsenbein, E. Amouyal, C. Adamo and F. Bedioui, *Chem.–Eur. J*., 2005, **11**, 3711; (*c*) J.-S. Yang, J.-L. Yan, C.-Y. Hwang, S.-Y. Chiou, K.-L. Liau, H.-H. G. Tsai, G.-H. Lee and S.-M. Peng, *J. Am. Chem. Soc*., 2006, **128**, 14109; (*d*) S. Woitellier, J. P. Launay and C. Joachim, *Chem. Phys*., 1989, **2-3**, 481.
14 When ligand 4d was treated with (en)Pd$(NO_3)_2$ in D_2O–1,4-dioxane-d_8, a triangular complex and small amount of square complex were self-assembled in almost the same ratio of that for Pt(II) analogues.
15 3D cage-like complexes with the same M_6L_4 geometry: M. Fujita, D. Oguro, M. Miyazawa, H. Oka, K. Yamaguchi and K. Ogura, *Nature*, 1995, **378**, 469.
16 A. B. Morgan, J. L. Jurs and J. M. Tour, *J. Appl. Polym. Sci*., 2000, **76**, 1257.
17 M. J. Frisch, G. W. Trucks, H. B. Schlegel, G. E. Scuseria, M. A. Robb, J. R. Cheeseman, J. A. Montgomery, Jr., T. Vreven, K. N. Kudin, J. C. Burant, J. M. Millam, S. S. Iyengar, J. Tomasi, V. Barone, B. Mennucci, M. Cossi, G. Scalmani, N. Rega, G. A. Petersson, H. Nakatsuji, M. Hada, M. Ehara, K. Toyota, R. Fukuda, J. Hasegawa, M. Ishida, T. Nakajima, Y. Honda, O. Kitao, H. Nakai, M. Klene, X. Li, J. E. Knox, H. P. Hratchian, J. B. Cross, V. Bakken, C. Adamo, J. Jaramillo, R. Gomperts, R. E. Stratmann, O. Yazyev, A. J. Austin, R. Cammi, C. Pomelli, J. Ochterski, P. Y. Ayala, K. Morokuma, G. A. Voth, P. Salvador, J. J. Dannenberg, V. G. Zakrzewski, S. Dapprich, A. D. Daniels, M. C. Strain, O. Farkas, D. K. Malick, A. D. Rabuck, K. Raghavachari, J. B. Foresman, J. V. Ortiz, Q. Cui, A. G. Baboul, S. Clifford, J. Cioslowski, B. B. Stefanov, G. Liu, A. Liashenko, P. Piskorz, I. Komaromi, R. L. Martin, D. J. Fox, T. Keith, M. A. Al-Laham, C. Y. Peng, A. Nanayakkara, M. Challacombe, P. M. W. Gill, B. G. Johnson, W. Chen, M. W. Wong, C. Gonzalez and J. A. Pople, *GAUSSIAN 03 (Revision C.02)*, Gaussian, Inc., Wallingford, CT, 2004.

